20

Shaw, J. H., E. Novoa, and C. D. Connors, 2004, Structural controls on growth stratigraphy in contractional fault-related folds, *in* K. R. McClay, ed., Thrust tectonics and hydrocarbon systems: AAPG Memoir 82, p. 400–412.

Structural Controls on Growth Stratigraphy in Contractional Fault-related Folds

John H. Shaw

Dept. of Earth & Planetary Sciences, Harvard University, Cambridge, Massachusetts, U.S.A.

Enrique Novoa

Departamento de Ciencia de La Tierra, Gerencia de Produccion y Exploracion, PDVSA-INTEVEP, Los Teques, Estado Miranda, Venezuela

Christopher D. Connors[1]

Texaco Exploration, Bellaire, Texas, U.S.A.

ABSTRACT

We describe local structural controls on deposition above contractional fault-related folds that yield patterns of stratigraphic onlaps, pinch-outs, and facies transitions that are diagnostic of folding mechanism. In folds that grow by kink-band migration, stratigraphic onlaps and pinch-outs that formed at emergent fold scarps are incorporated into fold limbs and aligned along growth axial surfaces. In contrast, the positions of these same features in structures that grow primarily by limb rotation are more variable and are controlled directly by sedimentation-to-uplift ratio. We present kinematic models and natural examples that integrate seismic reflection data and well control to describe these structural influences on growth stratigraphy. An understanding of this interplay between local deformation and deposition helps us infer the positions of subtle pinch-outs that may provide hydrocarbon traps and can yield a detailed history of structural development.

INTRODUCTION

Patterns of deformed growth strata record the timing and kinematics of deformation, much as magnetic anomalies record the process of sea-floor spreading (Suppe et al., 1992). Thus, growth strata are commonly used to define the ages and rates of deformation as well as to infer folding mechanisms (Medwedeff, 1989; Shaw and Suppe, 1994, 1996; Hardy et al., 1996; Vergés et al., 1996; Schneider et al., 1996; Ford et al., 1997; Suppe et al., 1997; Novoa et al., 2000).

Deformation also can influence the internal stratigraphy of growth strata. In cases where uplift rate locally exceeds sedimentation rate, folding and faulting can produce surface scarps that control sediment accommodation space and influence local depositional systems

[1]*Present address*: Dept. of Geology, Washington and Lee University, Lexington, Virginia, U.S.A.

(Burbank et al., 1996). For example, fan deposits may be ponded behind scarps, whereas the path of channels may be diverted to run parallel to the strike of the structures (Figure 1). These processes yield deposits restricted to one side of a fold or fault scarp. These deposits can be expressed as seismic sequences that onlap fold limbs, and in certain depositional environments may correspond to abrupt changes in sedimentary facies. In deep marine environments, for example, sand-rich fan and channel deposits may be restricted to the structurally low side of the scarps, whereas deposition on the fold crests may be dominated by hemipelagic muds. This would produce abrupt facies transitions across fold limbs. These stratigraphic patterns, consisting of onlapping growth sequences and sand pinch-outs on the flanks of structural highs, are commonplace. Yet, they are often modified by subsequent folding, which obscures the original depositional geometries. Two mechanisms— kink-band migration and limb rotation— are commonly employed to model the kinematics of this folding. Both mechanisms produce distinctly different patterns of deformed pinch-outs, onlaps, and facies boundaries in growth strata. We present kinematic models and natural examples to illustrate how these stratigraphic patterns form and are obscured by deformation via kink-band migration and limb rotation. Our intent is to show that both the internal stratigraphy and geometry of growth strata can be diagnostic of folding mechanisms. Conversely, we demonstrate that fold kinematics may influence the local distribution of sedimentary facies in a growth structure.

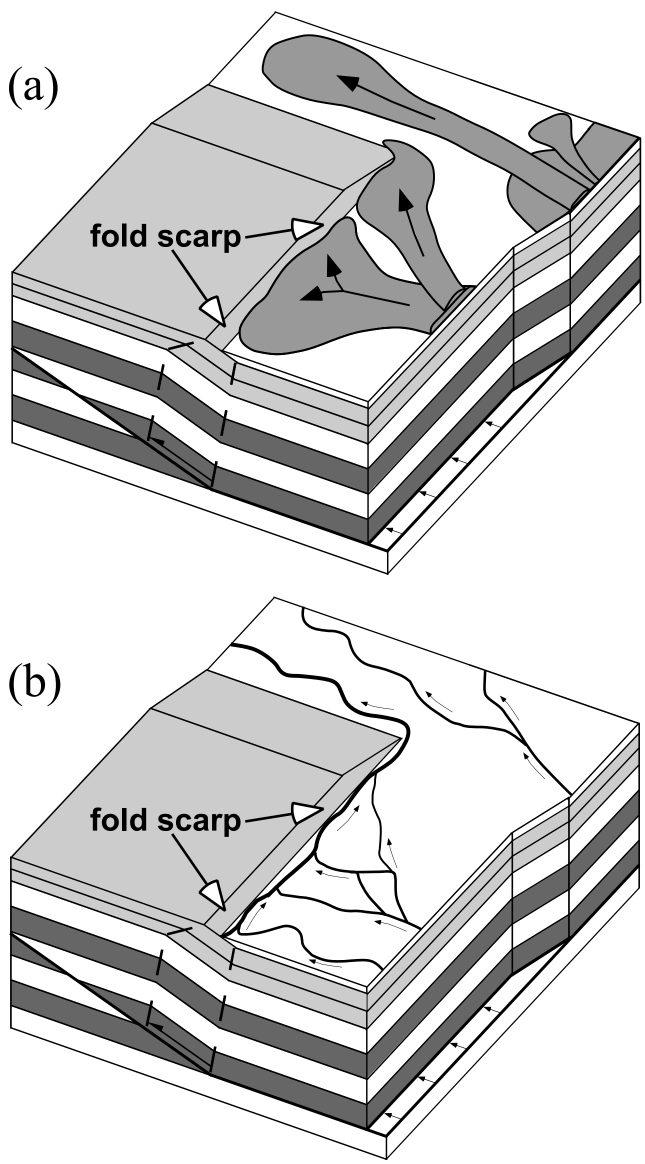

FIGURE 1. Perspective views of three-dimensional fault-bend fold models, showing the influence of emergent fold scarps on the distribution of growth sediments. (a) Ponding of fan deposits behind a fold scarp. (b) Deflection of channels to run along strike of the fold scarp.

MODELED STRATIGRAPHIC PATTERNS IN GROWTH STRUCTURES

In fault-related folds that develop purely by kink-band migration, fold limbs widen through time while maintaining a fixed dip (Suppe et al., 1992). Material is incorporated into the fold limb by passing through an active axial surface, which at depth is generally pinned to a bend or tip of a fault (Suppe, 1983; Suppe and Medwedeff, 1990). In cases where fold uplift rate exceeds syntectonic sedimentation rate, each increment of folding produces a discrete fold scarp located where the active axes project to the surface. Subsequent deposits then onlap the fold scarp, producing stratigraphic pinch-outs above the fold limb. In cases where anticlinal axial surfaces are active, growth strata remain undeformed and successive pinch-outs migrate up dip toward the anticlinal axis (Figure 2). In contrast, when synclinal axial surfaces are active, fold scarps and stratigraphic pinch-outs are displaced laterally and folded as they are incorporated into widening limbs (Suppe et al., 1992). Growth horizons between the positions of the onlaps and the active axial surface are folded concordantly with the underlying strata. New scarps form at the surface above the active, synclinal axial surfaces. Filling of each new accommodation space, followed by repeated folding and deposition, yields a series of stratigraphic pinch-outs at ‘‘paleoscarps’’ extending downward into the growth structure. These pinch-outs align along the fold’s growth axial surface (Figure 2), which marks the particles originally deposited along the active fold hinge and subsequently incorporated into the fold limb (Suppe et al., 1992). Thus growth axial surfaces, which often

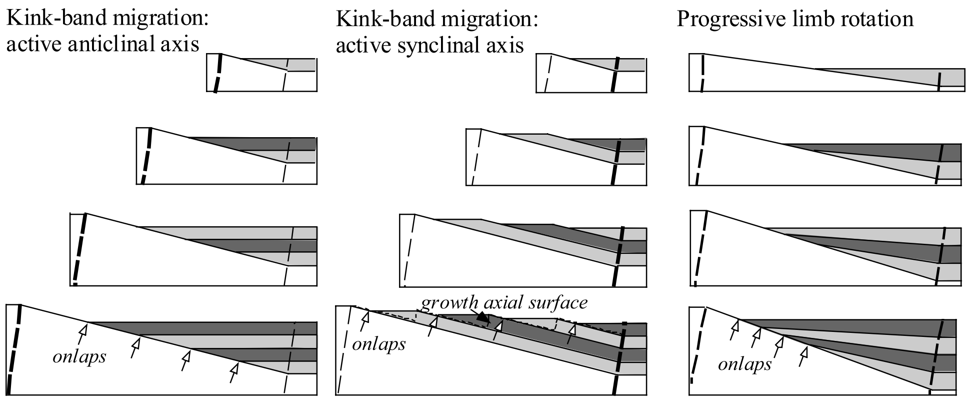

FIGURE 2. Kinematic models illustrating the onlap patterns in growth folds that develop by kink-band migration and limb rotation. In both of the kink-band-migration models, the sedimentation-to-uplift ratio is 0.75. In the limb-rotation model, the sedimentation rate is held constant while the uplift rate decreases as a function of the limb rotation (Hardy and Poblet, 1994).

correspond to a marked change in bed dip, can delineate these stratigraphic pinch-outs and associated facies boundaries in folds developed by kink-band migration.

Different stratigraphic patterns are expected in folds that grow primarily by limb rotation with fixed hinges (Figure 2), including certain types of detachment (Dahlstrom, 1990; Hardy and Poblet, 1994; Poblet et al., 1997; Storti and Poblet, 1997) and trishear (Erslev, 1991; Hardy and Ford, 1997; Allmendinger, 1998) folds. In these structures, rotation is distributed across the entire fold limb, with each increment of deformation. Thus fold scarps are diffuse, rather than being localized along active axial surfaces, as is the case in kink-band migration folds. Lacking discrete fold scarps, the positions of stratigraphic pinch-outs along rotational fold limbs are controlled primarily by the sedimentation-to-uplift ratio (Hardy et al., 1996; Storti and Poblet, 1997) and not by the positions of active axial surfaces, as is the case in kink-band migration folds. Hardy and Poblet (1994) demonstrated that in fixed-axis, limb-rotation models with sedimentation-to-uplift ratios nearly equal to one, pinch-outs form near anticlinal axial surfaces and corresponding growth horizons exhibit a fanning of limb dips. When sedimentation-to-uplift ratios are less than one, onlaps or pinch-outs form on the fold limb between the bounding axial surfaces (Figure 2). Uplift rates in these folds generally decrease through time, at constant shortening rates (Hardy and Poblet, 1994). Thus, when sedimentation rates are constant, onlapping growth horizons generally migrate up dip toward the anticlinal axial surface. In cases of increasing sedimentation rate relative to shortening rate, the onlaps will also tend to migrate upward toward the anticlinal axis. Onlaps will migrate toward the synclinal axis of a fold limb only when sedimentation rate relative to shortening rate is very low or decreases substantially through time.

The simple, end-member models shown in Figure 2 demonstrate that onlap patterns vary substantially between kink-band migration and limb-rotation folds, at constant rates of sedimentation and shortening. In natural cases, however, sedimentation and tectonic rates may vary over the life of folds. These variations can complicate onlap patterns. Thus, to distinguish fold kinematics, onlap relations should be considered in combination with the overall geometry of growth folds. For example, a kink-band migration fold with an active synclinal axis will preferentially form onlaps at fold scarps that develop where the synclinal axis meets the land surface. These onlaps are subsequently translated away from the synclinal axis by fold growth. As a result, onlaps generally migrate upward in section, toward the synclinal axis. Moreover, these onlaps are localized along dip changes in their corresponding stratigraphic horizons, where beds change from having primary sedimentary dip to being parallel to the underlying fold limb. This dip change defines the fold's growth axial surface and is not expected to occur in folds developed solely by limb rotation. Thus, patterns of onlaps migrating toward synclinal axes, combined with marked bed-dip changes and narrowing-upward, parallel fold geometries in growth strata, may be considered diagnostic of folding by kink-band migration with active synclinal axes. In contrast, a limb-rotation fold with constant sedimentation rate relative to shortening rate will typically have onlaps that migrate upward toward the anticlinal axis. This onlap pattern is similar to that of a kink-band migration fold with an active anticlinal axis. However, in growth, the kink-band migration structure does not exhibit a fanning of limb dips like that which is present in a limb-rotation structure (Figure 2). Thus, patterns of onlaps migrating toward anticlinal axes, combined with a shallowing-upward geometry of limb dips in growth strata, may together be considered diagnostic of folding by limb rotation. In the following section, we use these contrasting patterns of onlaps and fold geometry to interpret folding mechanisms in natural examples of both kink-band migration and limb-rotation structures. In the final example, we also compare these macroscopic fold patterns with sedimentary facies transitions observed in wells.

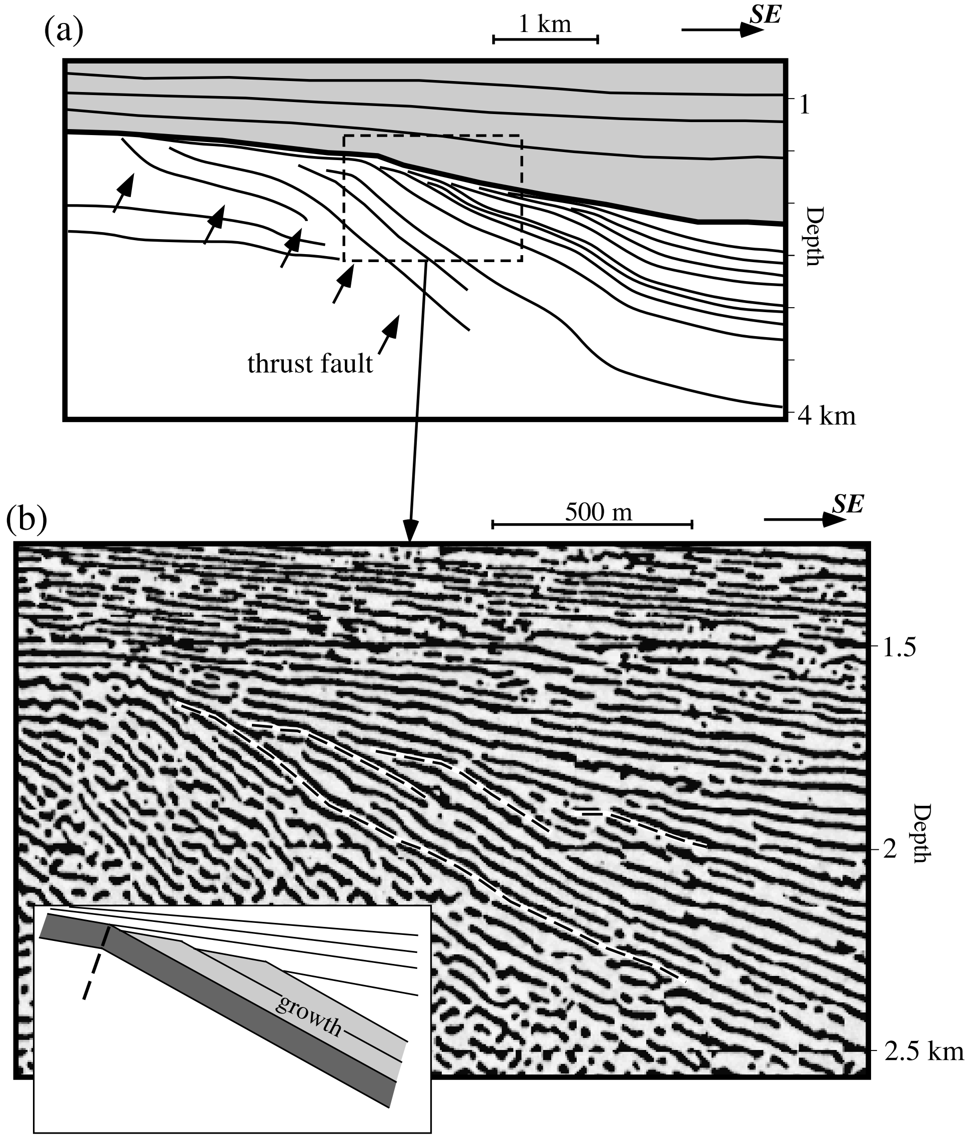

FIGURE 3. (a) Folded growth strata on the limb of an anticline interpreted on a seismic image from the western Jungar Basin, China. (b) 3-D prestack, depth-migrated seismic-reflection data (Zhang et al., 1996) imaging onlaps within the growth section. Highlighted growth sequences onlap the fold limb. To the east, these growth sequences change dip, becoming parallel with the underlying limb. This growth pattern is analogous to that modeled for folding by kink-band migration with an active synclinal axis (Figure 2 and inset). Younger strata above the onlapping growth units may record post-tectonic drape or a later phase of structural growth involving a component of limb rotation.

OBSERVED STRATIGRAPHIC PATTERNS IN GROWTH STRUCTURES

Jungar Basin, China

Stratigraphic sequences that onlap a fold limb are resolved in a prestack-migration, three-dimensional seismic survey (Figure 3) from the Jungar Basin, Xingjiang Province, northwestern China (Zhang et al., 1996). The stratigraphic section consists of alternating coarse- and fine-grained Mesozoic continental deposits that onlap an east-dipping fold limb at the western margin of the basin. The basin margin is defined by a southeast-vergent fold-and-thrust belt of Mesozoic age that holds large oil reserves in faulted and folded Jurassic and Triassic sandstones (Fan, 1991).

In the imaged structure, the onlaps migrated upward and laterally toward the synclinal axis of the fold (Figure 3). These growth strata dip gently as they onlap the fold limb, yet downdip, each growth unit is folded parallel to the underlying limb. We discount that these features might be clinoforms or related sedimentary features (Mitchum et al., 1977), because the beds dip more than 25°. Rather, we interpret the pattern of onlaps and the fold geometry of each of these growth horizons to reflect folding by kink-band migration with an active synclinal axis, as shown in Figure 2.

Each onlapping sequence in the Jungar example is about 100 m thick, and thus the fold scarps must have been at least this high. Moreover, each onlapping sequence must have been deposited during a period of little or no folding to yield the observed growth pattern. Without precise age control, we cannot determine the time it took to form such scarps or to fill the local accommodation space with sediment. Nevertheless, we can constrain these time periods by considering reasonable rates of uplift. Assuming very high rates of uplift (10 mm/yr), each scarp must have taken 10,000 years to form. Perhaps more reasonable uplift rates of 1 mm/yr

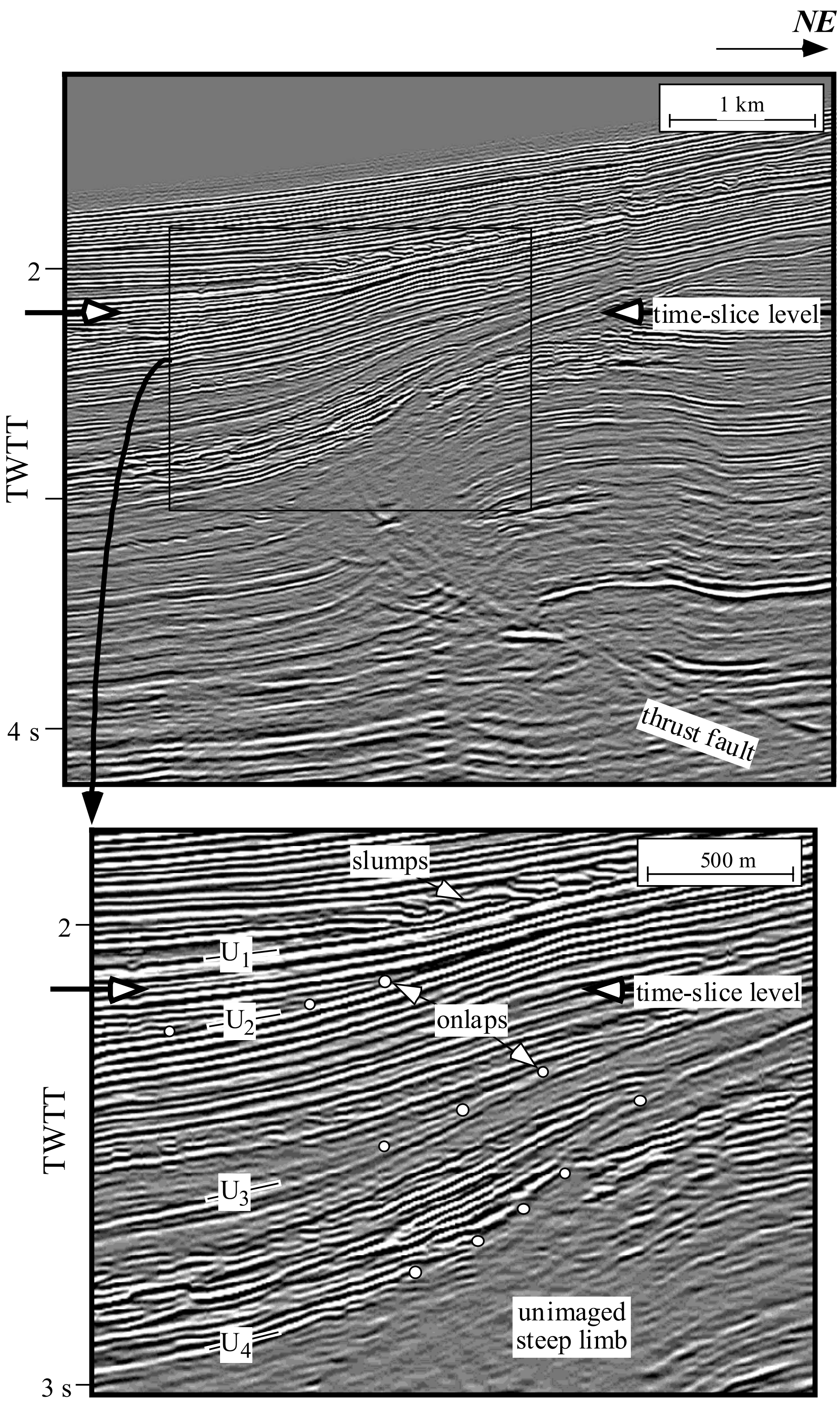

Figure 4. Migrated seismic-reflection profile imaging growth strata on the forelimb of a fault-related anticline, Niger Delta. Growth sequences are bounded by unconformities U1 through U4, and exhibit internally concordant bedding. Upward shallowing of bed dips reflects periods of fold amplification by limb rotation between the periods of deposition for each of these growth sequences. Onlaps at three of the major unconformities migrate upward toward the anticlinal axis of the fold, comparable with the limb rotation model of Figure 2. The time-slice level indicates the position of the map-view image shown in Figure 7.

or less would require 100,000 years or more for scarp formation. This implies that long (≥ 10,000 yr) periods of tectonic activity with little or no deposition alternated with periods of rapid deposition and/or tectonic quiescence during the formation of this fold.

Niger Delta

A poststack, three-dimensional seismic image resolves the forelimb of a contractional fault-related fold developed above a toe thrust in the deep-water Niger Delta (Figure 4). The thrust ramps upward from a basal detachment in the Acata Formation, a hemipelagic marine shale that overlies oceanic crust. Thrusting and related contractional folding consume slip on the detachment that was produced by gravity-driven extension and slumping on the continental shelf (Figure 5) (Lehner and de Ruiter, 1977; Doust and Omatsola, 1990). Growth strata in the contractional folds typically consist of alternating muds and sands in channel and basin-floor fan deposits.

In contrast to the previous example, growth strata on the forelimb of this fold show evidence of progressive limb rotation. The growth strata are composed of

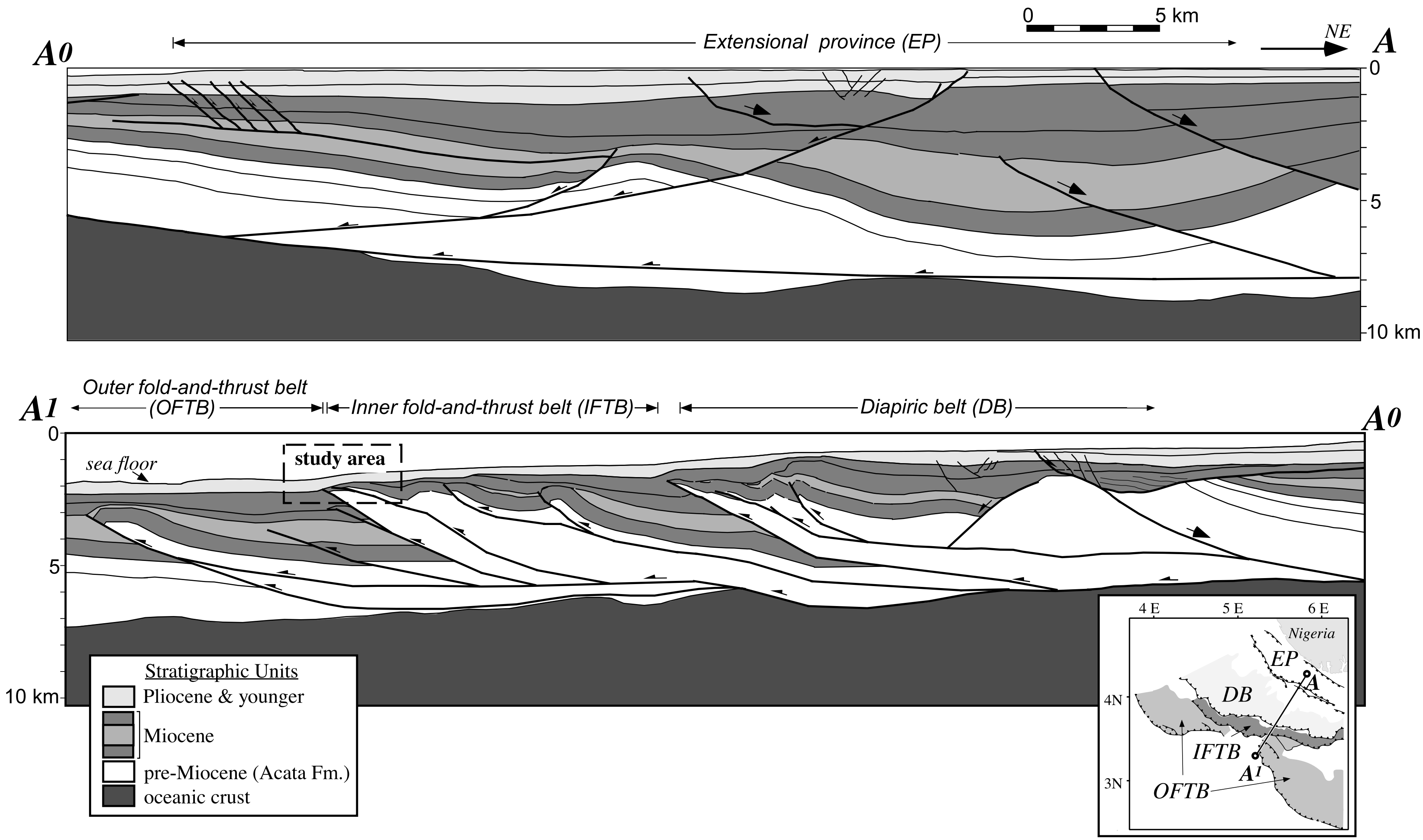

FIGURE 5. Regional geologic cross section across the Niger Delta, showing a detachment above oceanic crust that links extensional structures on the shelf to toe-thrust systems in deeper water. The structure shown in Figure 4 lies in the inner fold-and-thrust belt (IFTB).

several sequences, bounded by unconformities, that onlap the underlying fold limb. The dips of the sequences shallow upward, suggesting that the fold amplified between the deposition of each of these units. Pinch-outs, which are denoted by onlapping reflections, occur at the base of each major growth sequence. Pinch-outs migrate toward the anticlinal crest along each major unconformity, which is consistent with the pattern of onlaps expected for limb-rotation folds with constant or increasing rates of sedimentation relative to shortening (Figure 2). Notably, pinch-outs are not associated with prominent dip changes in their corresponding seismic horizons or in the underlying fold limb, as was the case in kink-band migration models (Figure 3). Thus, we interpret that this fold developed with a component of limb rotation.

The presence of several major unconformities with onlapping sequences reflects an episodic relationship between sedimentation and folding in this forelimb. Although the dips of sequences shallow upward, consistent with limb rotation, the bed dips within each sequence are roughly parallel. This pattern indicates that the fold did not simply amplify during the deposition of each sequence, but rather that it grew largely between the deposition of each sequence. Thus, the growth structure exhibits periods of very low sedimentation-to-uplift ratio alternating with periods of deposition in the absence of substantial deformation.

This growth history can be explained as a function of the forelimb's orientation relative to the direction of sediment transport (Burbank et al., 1996). The forelimb dips in the direction of regional sediment transport, which is southwest from the coast toward the abyssal plain (Doust and Omatsola, 1990). Thus, instead of sediments continuously ponding against the fold limb, sediment may, at times, have been restricted to the local accommodation space on the opposite side of the fold (i.e., above the backlimb). In effect, the forelimb occupied a depositional "shadow zone" behind the emergent anticline (Figure 6). Periods of rapid uplift of the fold crest would favor restriction of the sediment to the backlimb. Thus, periods of rapid fold amplification would correlate with periods of little or no deposition on the forelimb. In contrast, when uplift stopped or decreased substantially, the backlimb accommodation space would fill. Subsequently, sediments could breach the crest of the structure and be deposited on the forelimb (Figure 6). As is resolved in a three-dimensional seismic time slice, the onlapping sequences in this example are fan deposits fed by a canyon that breached the anticlinal crest (Figure 7). In this depositional scenario, forelimb deposits should correlate with periods of little or no uplift. This is consistent with the observation that the growth sequences exhibit no internal fanning of dips, as would be expected if they were deposited during limb rotation. In periods of rapid fold growth, sediments were generally not deposited on the forelimb. As a result, each depositional sequence has a distinctly shallower dip than that of the underlying sequence.

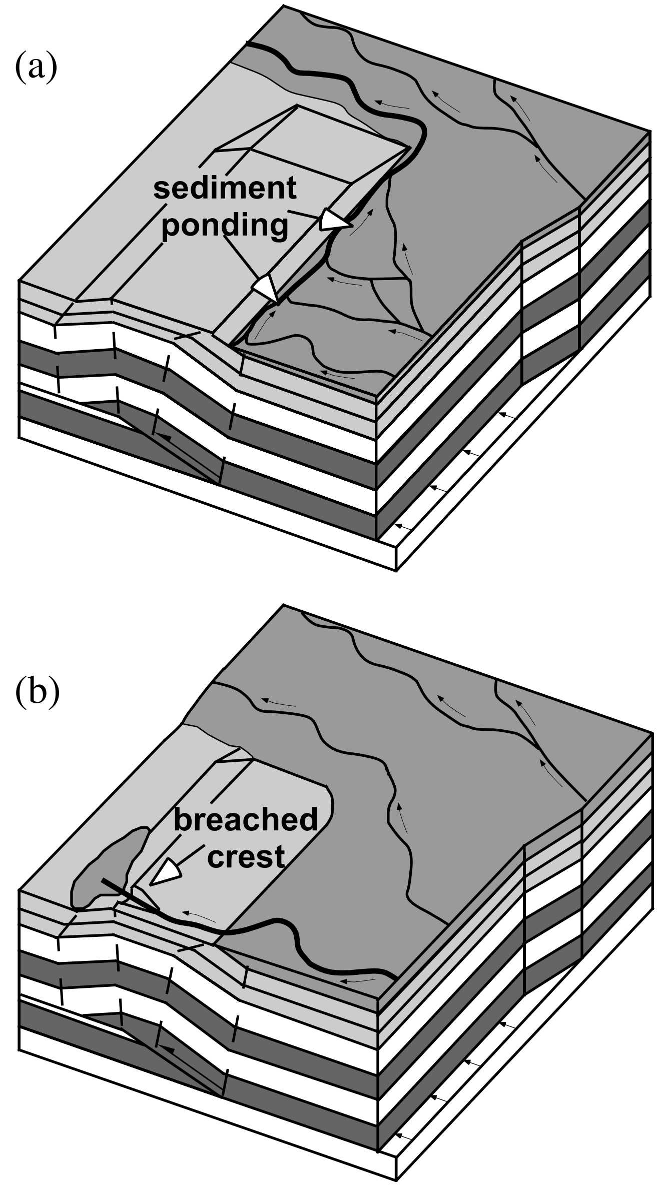

FIGURE 6. Perspective views of three-dimensional sequential models describing the depositional history proposed for the Niger Delta example shown in Figure 4. (a) Ponding of deposits behind a backlimb fold scarp restricts sediments to the backlimb accommodation space. No sediments are deposited above the forelimb. (b) After the backlimb accommodation space is filled, sediments are transported over the fold crest and deposited above the forelimb. Although a simple fault-bend fold structure formed by kink-band migration is shown, these general growth patterns also may occur in folds developed solely, or in part, by limb rotation.

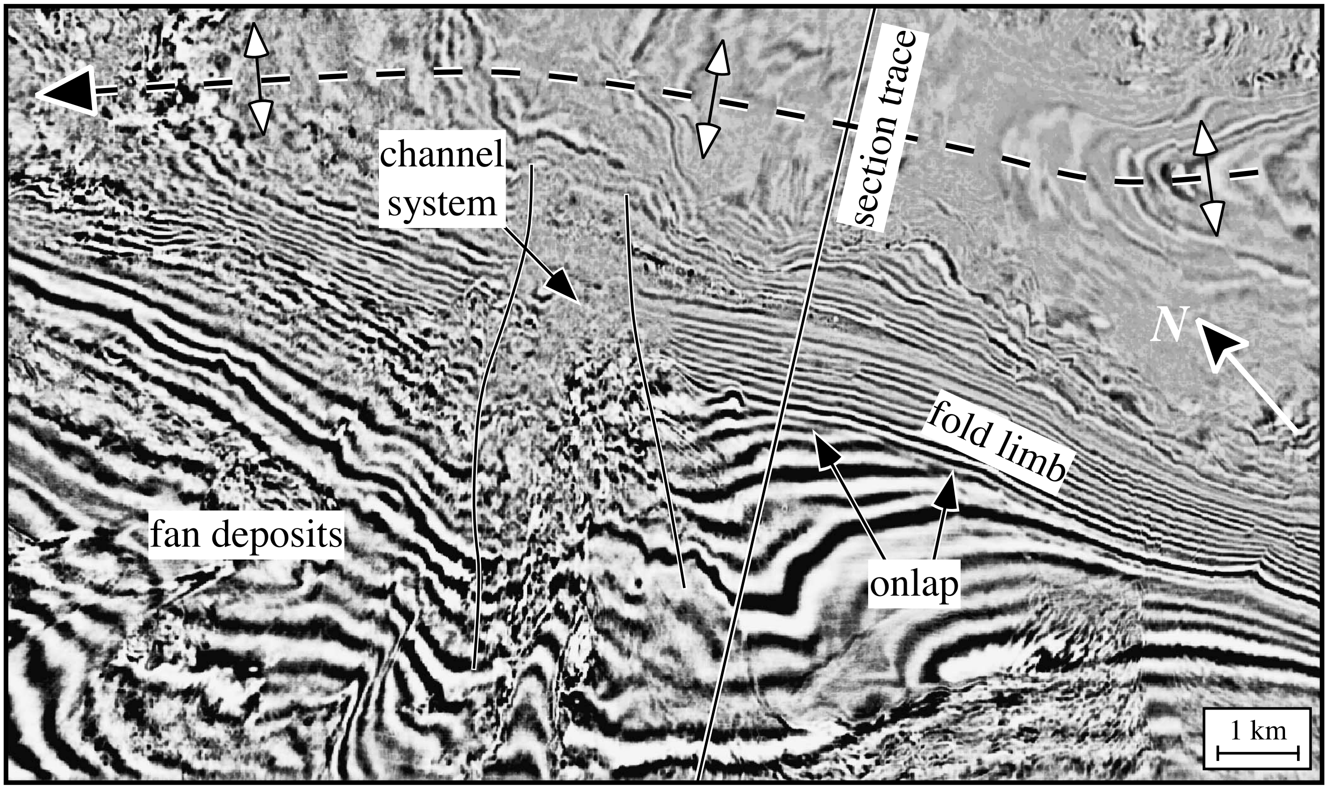

FIGURE 7. Three-dimensional seismic-reflection time slice across the growth anticline imaged in Figure 4. A southwest-flowing channel system breaches the anticlinal crest, producing fan deposits that onlap the forelimb. A series of these onlapping sequences imaged in Figure 4 records several distinct periods when the fold crest was breached by channel systems.

Transverse Ranges, California

Our final example is a Tertiary growth fold along the Offshore Oak Ridge trend in the Santa Barbara Basin, California (Figure 8). The basin is a southwestern extension of the Transverse Ranges Fold-and-thrust Belt of south-central California, which developed during Pliocene through Quaternary contraction (Yeats, 1983; Namson and Davis, 1988). Growth strata in the Offshore Oak Ridge structure contain thick sandstone sections interbedded with pelagic shales and turbidites (Sangree and Widmier, 1977). The fold exhibits an upward-narrowing limb that is interpreted to reflect folding by kink-band migration (Shaw and Suppe, 1994; Novoa et al., 1995, Novoa et al., 2000). No major stratigraphic onlaps on the fold limb are observed, however, at the resolution of the seismic image. Thus, we investigate the internal stratigraphy of the growth strata using well control to determine whether finer stratigraphy reflects the folding mechanism. We define the structural geometry and distribution of sedimentary facies in this fold using seismic-reflection images and well control, including dipmeter, sonic, spontaneous potential, and resistivity logs. The seismic profile in Figure 9 was depth converted using the sonic logs and stacking velocities. The seismic image closely correlates with posted dipmeter data in the wells. Thus, we suggest that the velocities and depth conversion are sound and provide an accurate picture of the structural geometry and precise ties of stratigraphy in the wells to the seismic image.

The distribution of sand and shale facies in the Pliocene-Quaternary Pico Formation of the Offshore Oak Ridge trend is defined by electric logs (Figure 9). The lower part of the middle Pico Formation contains mostly sandstones with thin shale partings, whereas the uppermost middle Pico and upper Pico sections consist almost entirely of shale. The intervening middle Pico section, however, contains a lateral change from sandstone- to shale-dominated facies across the Offshore Oak Ridge fold. Prominent sandstone intervals in well 1, between horizons S and X, are also present in the north-dipping fold limb (wells 2 and 4). However, these sandstones are absent on the fold crest (well 6) and to the south of the Oak Ridge trend. This facies change occurs abruptly across the growth axial surface (A′) of the Oak Ridge fold (Figure 9, inset), which is defined by the upward change from north-dipping to horizontal beds recorded in the seismic image and by dipmeter. The position of these pinch-outs along the growth axial surface, combined with the parallel dips of growth strata in the fold limb, are consistent with patterns modeled

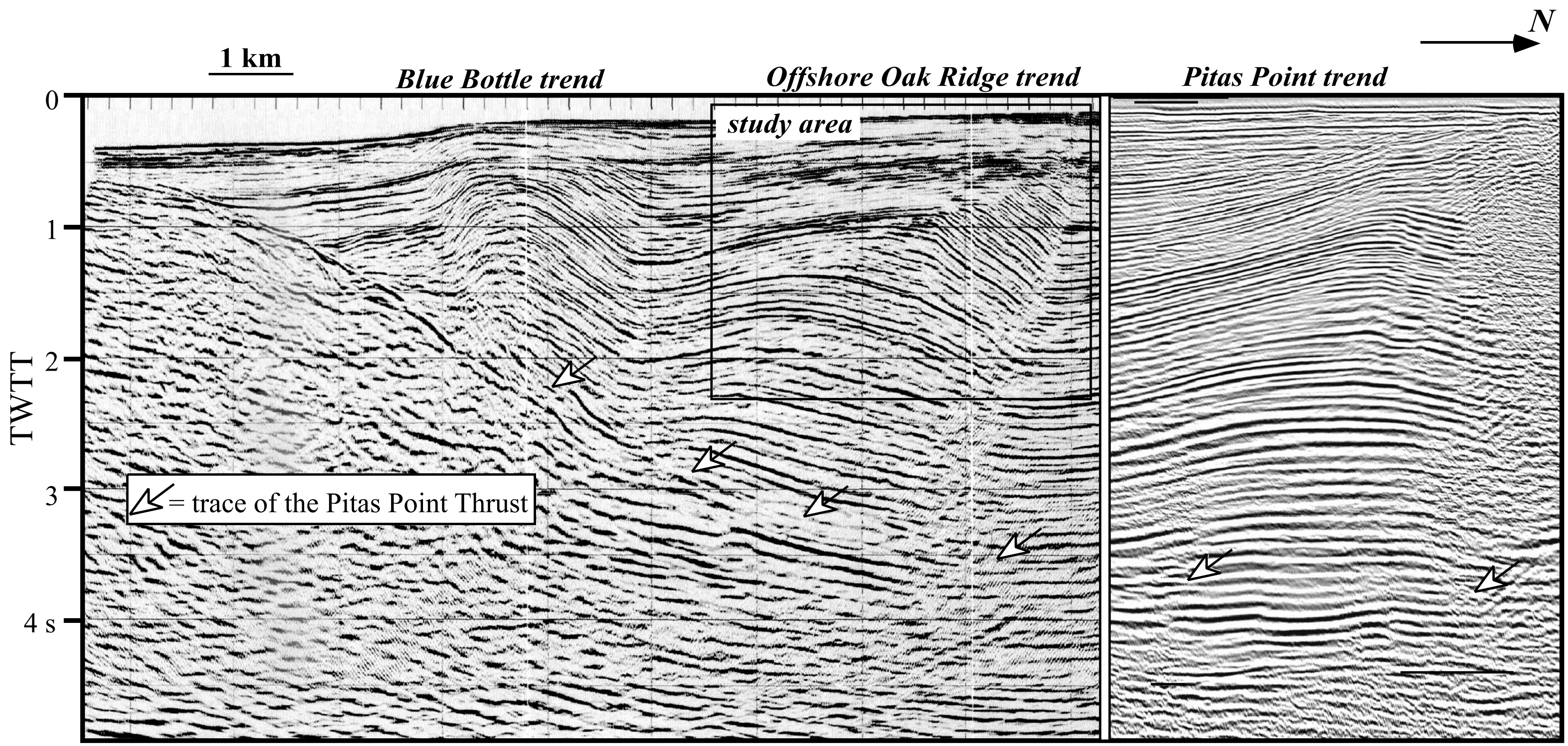

FIGURE 8. Three-dimensional, migrated seismic profiles across the eastern Santa Barbara Channel imaging a series of contractional growth folds, including the Offshore Oak Ridge structure (Shaw and Suppe, 1994; Shaw et al., 1996). The Offshore Oak Ridge structure developed above a series of vertically stacked blind-thrust faults, including the Pitas Point thrust. The position of the Pitas Point thrust is defined by reflector truncations and downward-terminating dip domains.

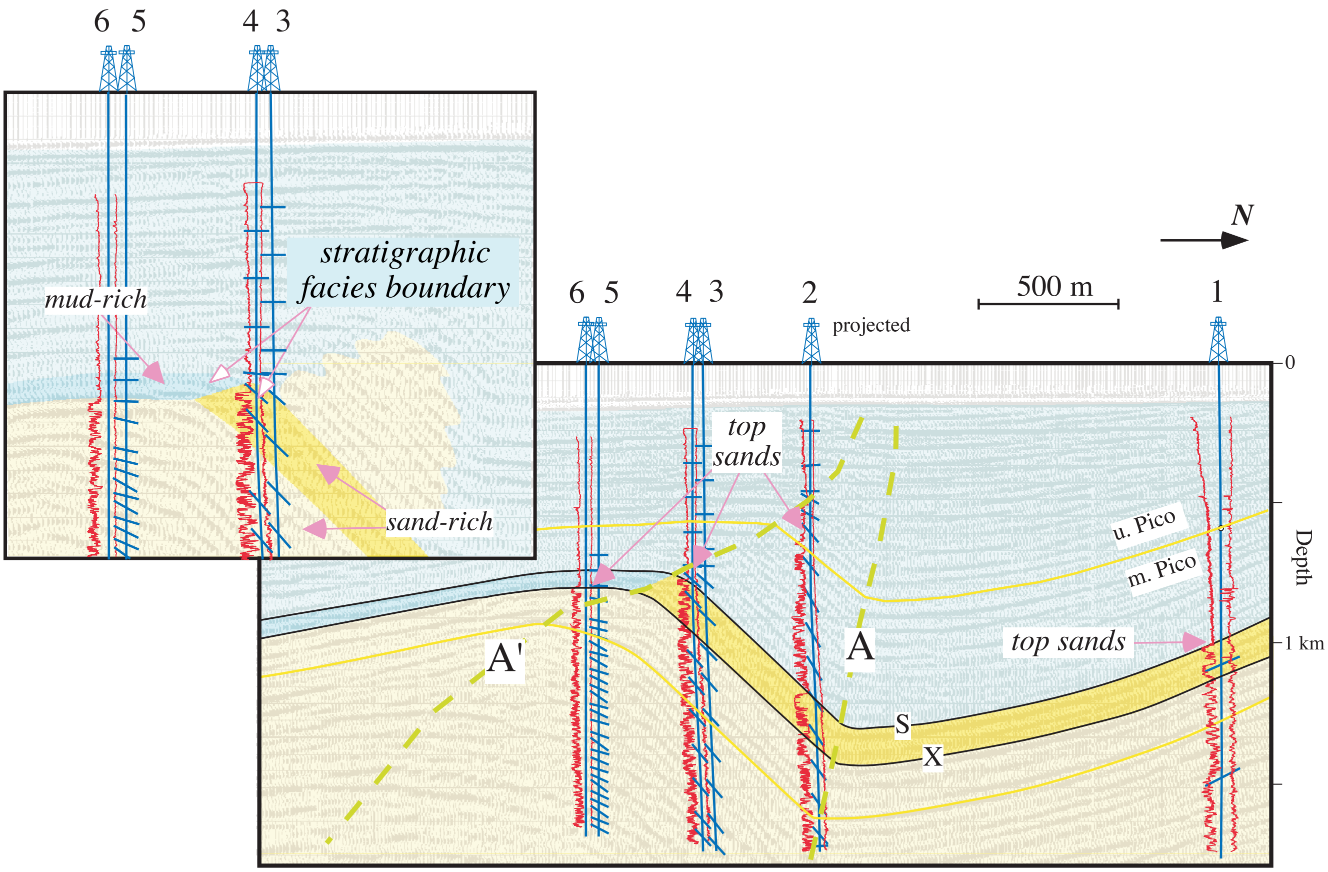

FIGURE 9. Structurally controlled facies change and sandstone pinch-outs on the Offshore Oak Ridge trend, Santa Barbara Channel, California, U.S.A. The migrated seismic-reflection profile is displayed in depth with a vertical exaggeration of 2:1. Spontaneous potential (SP) and resistivity logs are shown on the left and right sides, respectively, of selected wells. Shifts to the left in the SP logs indicate sands. Note how, in well 6, the uppermost sandstones in wells 1, 2, and 4 have changed to shale across the growth axial surface (A′). Enlarged section at left shows facies change across the growth axial surface. Wells: 1 = Texaco 234-7; 2 = Conoco SBC 21; 3 = Conoco SBC 34; 4 = Exxon SBC 39B; 5 = Arco SBC 39B; 6 = Phillips SBC 2. Data courtesy of the former Texaco, Chevron, and Arco.

by kink-band migration with an active synclinal axis (Figure 2). Thus, we suggest that the facies change was localized by ponding of turbidite sands behind the fold scarp (Figure 10). Subsequent folding by kink-band migration has translated these pinch-outs, which formed above the active axial surface A, to their present position near the anticlinal crest along the growth axial surface (A′).

Sandstone pinch-outs between horizons S and X occur in the uppermost part of the Pliocene turbidite sequence. This stratigraphic position correlates with a period of lower sediment influx, when deposits were unable to fill the local accommodation space produced by the fold scarp, as shown in Figure 1a. In contrast, older turbidite deposits overflowed the local accommodation space and thus are present on both sides of the fold (Figure 9). The apparent decrease in deposition rate, and/or increase in fold growth rate, is recorded in Figure 10 by the shape of the growth axial surface (A′), which shallows upward into the middle Pico section (Suppe et al., 1992; Shaw and Suppe, 1996).

Above horizon S, sandstones occur in well 2 that are not present to the north or south of the Offshore Oak Ridge trend (Figure 9). These discontinuous sands have a log character consistent with a more channelized facies than do the deeper ponded sands, and may be derived from submarine channel systems that were deflected to run along the base of the seafloor fold scarps (Figure 1b). The transition from turbidite- to channel-dominated deposits probably reflects a decrease in water depth caused by infilling of the basin, a trend that is well documented in other deep-water environments (Mitchum, 1985).

SUMMARY AND CONCLUSIONS

We have described how the internal stratigraphy and geometry of growth structures are influenced by the kinematics of fold growth. When sedimentation-to-uplift ratios are less than or equal to one, stratigraphic

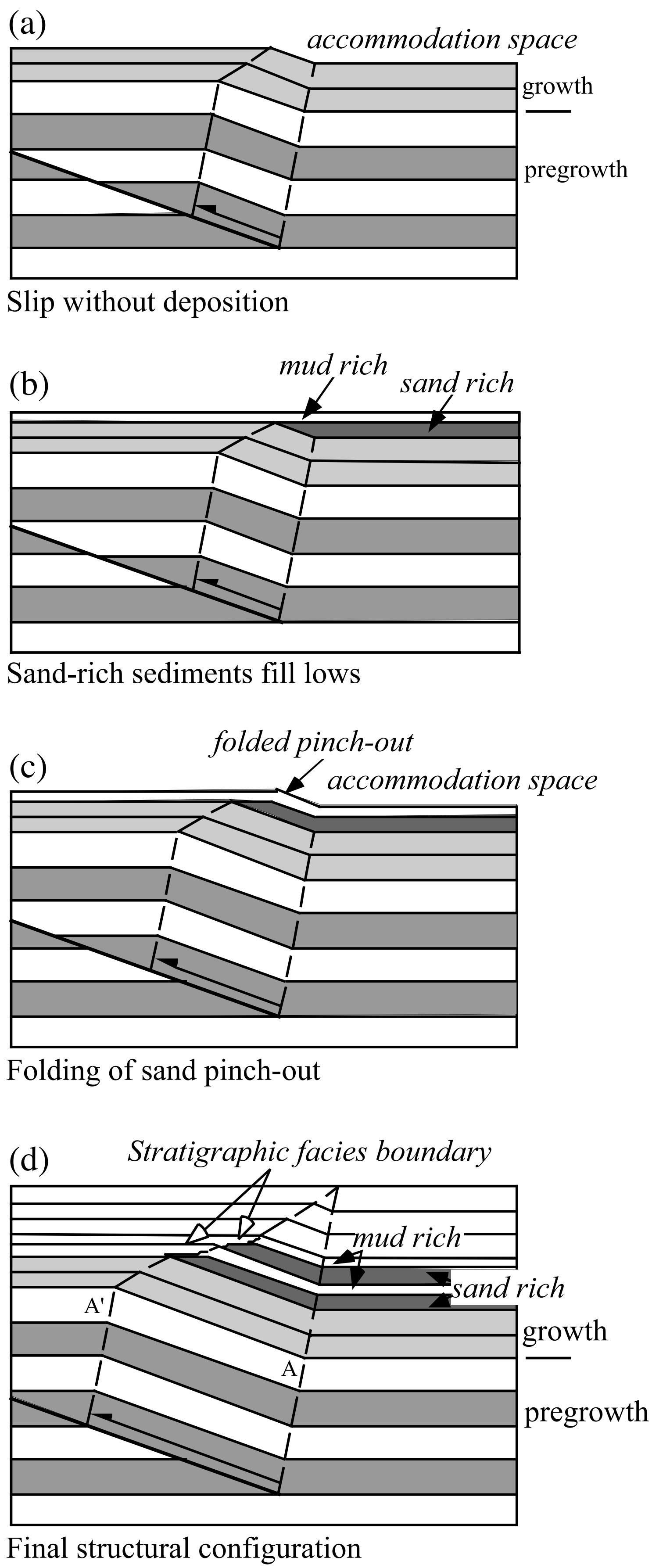

Figure 10. Sequential models illustrating the development of the Offshore Oak Ridge structure by kink-band migration and fault-bend folding with deposition. (a) Folding generates a surface scarp and local accommodation space. (b) Sand-rich deposits pond behind the fold scarp and fill the accommodation space, as described in Figure 1. After the accommodation space is filled, mud-rich sediments blanket the structure. (c) Another episode of folding generates a surface scarp and local accommodation space, which is subsequently filled with sand-rich deposits. The sandy units pinch out onto the fold limb. (d) Deformation folds and translates the sand pinch-outs, which are aligned along the axial surface A′. Muds are deposited concurrent with this last phase of deformation.

pinch-outs and associated facies transitions may develop on fold limbs. These simple stratigraphic patterns are modified by subsequent folding. In folds that develop by kink-band migration, onlaps and corresponding stratigraphic pinch-outs develop at discrete fold scarps associated with active axial surfaces. Progressive deformation folds and translates these onlaps, so that they are aligned with prominent dip changes that occur along the fold's growth axial surface (Suppe et al., 1992). In contrast, folds that develop purely by limb rotation have onlap patterns controlled primarily by the relative rates of sedimentation and deformation. In general, onlaps migrate toward the anticlinal hinge of the fold, in limb-rotation structures. Moreover, these onlaps are not associated with prominent dip changes in their corresponding stratigraphic horizons, as was the case for kink-bend migration structures. Thus, we can expect differences in the patterns of onlapping stratigraphic sequences, as well as in macroscopic fold geometry, between folds that develop by kink-band migration and those that develop by limb rotation. We used these insights to interpret that two folds, in southern California and China, developed by kink-band migration. In contrast, an example from Nigeria showed a growth fold that has amplified with a component of limb rotation.

In addition to distinguishing fold kinematics, insights into the internal stratigraphy of growth structures can help to resolve a detailed history of structural development. The large size (≈100 m) of fold scarps inferred in the example from China, and the punctuated limb rotations observed in the Nigeria example, suggest that relative rates of sedimentation and deformation varied substantially over the growth of these structures. These changes may reflect episodic sedimentation. However, they may also result from long periods of heightened tectonic activity followed by quiescence. In contrast, small scarps and pinch-outs (<2 m) in the Offshore Oak Ridge trend may reflect individual episodes of fold growth, perhaps driven by earthquake rupture on the underlying faults. Alternatively, the patterns could be generated by steady-state folding with episodic turbidite deposition. Detailed absolute-age control for the stratigraphic sections, combined with the observed fold patterns, would be needed to resolve between these sedimentological and tectonic influences. Both factors, however, clearly influence the geometry and internal stratigraphy of growth strata. All three of the examples that we document exhibit variable rates of tectonism and shortening, which may be common in contractional growth structures.

Stratigraphic facies changes and pinch-outs in growth structure also can provide hydrocarbon traps. Although these features can be observed directly in some seismic-reflection profiles (Figure 3), we demonstrate that they can exist beyond the imaging resolution of typical seismic-reflection data and thus must be corroborated by well control (Figure 9). Nevertheless, knowledge of the folding mechanism can be used to predict the local distribution of these traps in certain types of structures. For example, subtle pinch-outs can align along growth axial surfaces in folds that are formed by kink-band migration (e.g., fault-bend and fault-propagation folds), as illustrated by our example from California. These growth axial surfaces are readily observed on seismic images as marked changes in the dips of seismic reflections. Thus, macroscopic fold patterns can be used to identify areas that may offer stratigraphic traps, which could then be evaluated by subsequent drilling. These subtle traps can occur downdip on the flanks and limbs of structures. They are seldom tested by wells on the fold crest, and thus may provide exploration and development opportunities even in mature petroleum provinces.

ACKNOWLEDGMENTS

This research was supported by Texaco, Inc., and PDVSA, with data generously provided by Arco, Chevron, BP, Statoil, and Texaco. The authors thank John Suppe and Stephen Hook for helpful insights into growth folding and Kevin Bishop for assistance with processing of the seismic profile from California. Ken McClay and two anonymous reviewers provided helpful suggestions for improving the manuscript.

REFERENCES CITED

Allmendinger, R. W., 1998, Inverse and forward numerical modeling of trishear fault-propagation folds: Tectonics, v. 17, no. 4, p. 640–656.

Burbank, D., A. Meigs, and N. Brozovic, 1996, Interaction of growing folds and coeval depositional systems: Basin Research, 8, p. 199–223.

Dahlstrom, C. D. A., 1990, Geometric constraints derived from the law of conservation volume and applied to evolutionary models for detachment folding: AAPG Bulletin, v. 74, p. 336–344.

Doust, H., and E. Omatsola, 1990, Niger Delta, *in* J. D. Edwards and P. A. Santogrossi, eds., Divergent/passive margins: AAPG Memoir 48, p. 201–238.

Erslev, E. A., 1991, Trishear fault-propagation folding: Geology, v. 19, no. 6, p. 617–620.

Fan, C. L., 1991, Reservoir models in the Jungar Basin, Xin-jiang, north-west China: Marine and Petroleum Geology, v. 8, p. 107–114.

Ford, M., E. A. Williams, A. Artoni, J. Vergés, and S. Hardy, 1997, Progressive evolution of a fault-related fold pair from growth strata geometries, Sant Llorenç de Morunys, SE Pyrenees: Journal of Structural Geology, v. 19, no. 3–4, p. 413–441.

Hardy, S., and M. Ford, 1997, Numerical modeling of trishear fault-propagation folding and associated growth strata: Tectonics, v. 16, no. 5, p. 841–854.

Hardy, S., and J. Poblet, 1994, Geometric and numerical model of progressive limb rotation in detachment folds: Geology, v. 22, p. 371–374.

Hardy, S., J. Poblet, K. McClay, and D. Waltham, 1996, Mathematical modeling of growth strata associated with fault-related fold structures, *in* P. G. Buchanan and D. A. Nieuwland, eds., Modern developments in structural interpretation, Validation and modeling: Geological Society of London Special Publication 99, p. 265–282.

Lehner, P., and P. A. C. de Ruiter, 1977, Structural history of Atlantic margin of Africa: AAPG Bulletin, v. 61, p. 963–981.

Medwedeff, D. W., 1989, Growth fault-bend folding at southeast Lost Hills, San Joaquin Valley, California: AAPG Bulletin, v. 73, p. 54–67.

Mitchum, R. M., 1985, Seismic stratigraphic expression of submarine fans, *in* O. R. Berg and D. G. Woolverton, eds., Seismic stratigraphy II: An integrated approach to hydrocarbon exploration: AAPG Memoir 39, p. 274.

Mitchum, R. M., P. R. Vail, and S. Thompson III, 1977, Seismic stratigraphy and global changes of sea level, Part 2: The depositional sequence as a basic unit for stratigraphic analysis, *in* C. E. Payton, ed., Seismic stratigraphy— applications to hydrocarbon exploration: AAPG Memoir 26, 516 p.

Namson, J., and T. L. Davis, 1988, A Structural transect of the western Transverse Ranges, California: Implications for lithospheric kinematics and seismic risk evaluation: Geology, v. 16, p. 675–679.

Novoa, E., J. Suppe, K. Mueller, and J. Shaw, 1995, Axial surface mapping of active folds in the Santa Barbara Channel, *in* 1995 Thrust ramps and detachment faults in the Western Transverse Ranges: SCEC workshop Abs., p. 19.

Novoa, E., J. Suppe, and J. H. Shaw, 2000, Inclined-shear restoration of growth folds: AAPG Bulletin, v. 84, p. 787–804.

Poblet, J., K. McClay, F. Storti, and J. A. Muñoz, 1997, Geometries of syntectonic sediments associated with single layer detachment folds: Journal of Structural Geology, v. 19, p. 369–381.

Sangree, J. B., and J. M. Widmier, 1977, Seismic interpretation of clastic depositional facies, *in* C. E. Payton, ed., Seismic stratigraphy – applications to hydrocarbon exploration: AAPG Memoir 26, 516 p.

Schneider, C. L., C. Hummon, R. S. Yeats, and G. L. Huftile, 1996, Structural evolution of the northern Los Angeles basin, California, based on growth strata: Tectonics, v. 15, p. 341–355.

Shaw, J., and J. Suppe, 1994, Active faulting and growth folding in the eastern Santa Barbara Channel, California: Bulletin of the Geological Society of America, v. 106, p. 607–626.

Shaw, J., and J. Suppe, 1996, Earthquake hazards of active blind-thrust faults under the central Los Angeles basin, California: Journal of Geophysical Research, v. 101, p. 8623–8642.

Shaw, J. H., S. C. Hook, and J. Suppe, 1996, Structural trend analysis by axial surface mapping: Reply to Discussion of Shaw, J. H., S. Hook, and J. Suppe, 1994, Structural trend analysis by axial surface mapping in AAPG Bulletin, v. 78, p. 700–721: AAPG Bulletin, v. 80, p. 780–787.

Storti, F., and J. Poblet, 1997, Growth stratal architectures associated with decollement folds and fault-propagation folds: Inferences on fold kinematics: Tectonophysics, v. 282, p. 353–373.

Suppe, J., 1983, Geometry and kinematics of fault-bend folding: American Journal of Science, v. 283, p. 684–721.

Suppe, J., and D. A. Medwedeff, 1990, Geometry and kinematics of fault-propagation folding: Eclogae Geologicae Helvetiae , v. 83, p. 409–454.

Suppe, J., G. T. Chou, and S. C. Hook, 1992, Rates of folding and faulting determined from growth strata, *in* K. R. McClay, ed., Thrust tectonics: London, Chapman & Hall, p. 105–121.

Suppe, J., F. Sàbat, J. A. Muñoz, J. Poblet, E. Roca, and J. Vergés, 1997, Bed-by-bed growth by kink-band migration: Sant Llorenç de Morunys, Eastern Pyrenees: Journal of Structural Geology, v. 19, p. 443–461.

Vergés, J., D. W. Burbank, and A. Meigs, 1996, Unfolding: An inverse approach to fold kinematics: Geology, v. 24, no. 2, p. 175–178.

Yeats, R. S., 1983, Large-scale Quaternary detachments in Ventura basin, southern California: Journal of Geophysical Research, v. 88, no. B1, p. 569–583.

Zhang, G., L. Liu, and Z. Wu, 1996, The preliminary application of GeoDepth prestack depth migration in data processing in Xinjiang area: Proceedings of the 1996 International Geophysical Conference, Society of Exploration Geophysicists/Chinese Society of Petroleum Geophysicists, Urumqi, P.R.C, p. 51–56.